Melt Polycondensation Approach for Reduction Degradable Helical Polyester Based on L-Cystine

Santhanaraj Anantharaj, Manickam Jayakannan

Department of Chemistry, Indian Institute of Science Education and Research (IISER)-Pune, Dr. Homi Bhabha Road, Pune, Maharashtra 411008, India
Correspondence to: M. Jayakannan (E-mail: jayakannan@iiserpune.ac.in)

Received 18 March 2016; accepted 13 May 2016; published online 29 June 2016
DOI: 10.1002/pola.28172

ABSTRACT: Melt polycondensation approach is developed for new classes of reduction responsive disulfide containing functional polyesters based on L-cystine amino acid resources under solvent free process. L-Cystine was converted into multifunctional ester-urethane monomer and subjected to thermoselective transesterification at 120 °C with commercial diols in the presence of $Ti(OBu)_4$ to produce polyesters with urethane side chains. The polymers were produced in moderate to high molecular weights and the polymers were found to be thermally stable up to 250 °C. The β-sheet hydrogen bonding interaction among the side chain urethane unit facilitated the self-assembly of the polyester into amyloid-like fibrils. The deprotection of urethane unit into amine functionality modified the polymers into water soluble cationic polyester spherical nanoparticles. The reduction degradation of disulfide bond was studied using DTT as a reducing agent and the high molecular weight polymers chains were found be chopped into low molecular weight oligomers. The cytotoxicity of cationic disulfide nanoparticle was studied in MCF-7 cells and they were found to be biocompatible and non-toxic to cells upto 50 μg/mL. The custom designed reduction degradable and highly biocompatible disulfide polyesters from L-cystine are useful for futuristic biomedical applications. © 2016 Wiley Periodicals, Inc. J. Polym. Sci., Part A: Polym. Chem. **2016**, *54*, 2864–2875

KEYWORDS: amino acids; melt polycondensation; Polycondensation; Polyesters; redox polymers; Self-assembly; stimuli-sensitive polymers; transesterification

INTRODUCTION Macromolecular architectures with disulfide chemical linkages are emerging as important polymeric materials for diverse application in thermoplastic and biomedical industry due to their excellent responsiveness to light, heat, pH, redox reagents, and enzymes.[1–4] The disulfide linkage in the polymer chains can be introduced via ring-opening polymerization of cyclic oligo-disulfides[5–10] or oxidative polymerization of thiol end-capped oligo-ethylene glycols (or PEGs).[11,12] Recently, photo-induced disulfide metathesis polymerization was developed to make hybrid polymers and photo-mendable polymeric materials.[13–15] Telechelic poly(disulfide)s were made by carefully controlling the stoichiometric balance between di-thiols and dithiopyridines.[16,17] Non-sulphur mediated or indirect methodologies were also reported for disulfide containing macromolecular architectures. Disulfide containing TEMPO initiator for polystyrene,[18] hyperbranched polymers,[19] and star copolymers via RAFT route[20,21] and ATRP for branched poly(t-butyl acrylate)s[22,23] are some of the important examples. Ring opening polymerization of disulfide cyclic derivatives produce reduction degradable linear polycarbonate,[24] hyperbranched polyglycerols,[25] and self-healing polymers.[14,26] Among the natural L-amino acid resources, L-cysteine has thiol (-SH) functionality and it readily oxidized into stable disulfide dimer L-cystine. N-carboxyl anhydrides of L-cystine[27–29] and L-methionine[30] monomers were subjected to ring opening polymerization to produce star shaped polymers and functional polypeptides, respectively. Very recently, L-cystine diamine was polymerized with fatty dicarboxylic acids in solution polycondensation route to make poly(disulfide amide) nanoparticles for docetaxel delivery.[31] These amino acid-based poly(disulfide)s were used as nanoscaffolds for delivering anticancer drugs[32–39] and gene.[40] These examples clearly envisage the importance of the disulfide polymers as reduction degradable thermoplastics and also as useful scaffold material for biomedical applications.

Melt polycondensation is an important synthetic methodology that is largely used for the manufacture of thermoplastic engineering polymers such as polyesters, polyamides, and polycarbonates.[41] Unfortunately, no effort has been taken until now for making disulfide linkage polymers based on the melt polycondensation chemistry in the literature. Hence,

Additional Supporting Information may be found in the online version of this article.

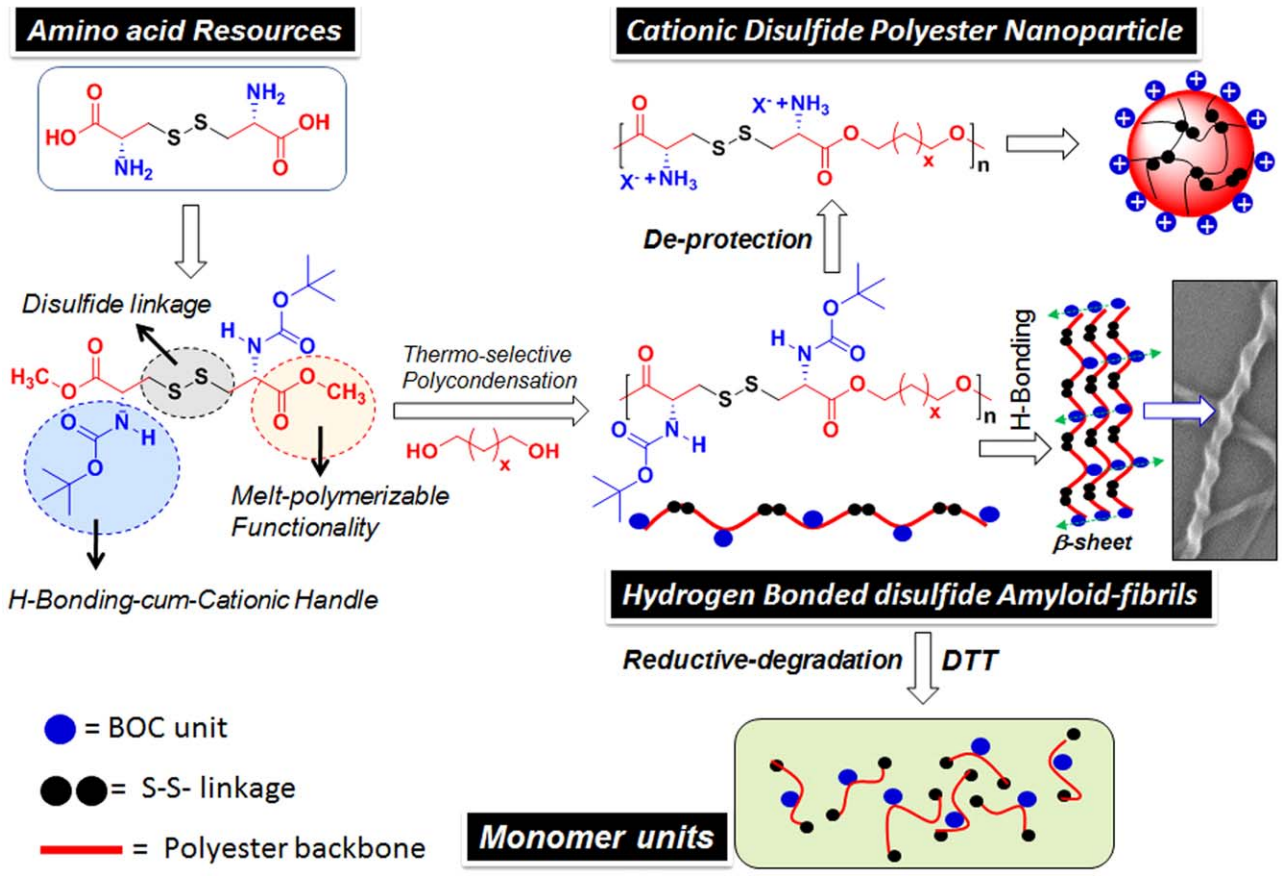

FIGURE 1 Approaches to develop reduction-degradable helical disulfide containing polyesters based on L-cystine amino acid resources. [Color figure can be viewed in the online issue, which is available at wileyonlinelibrary.com.]

the development of solvent free melt process for disulfide linkage polymer would provide new opportunity for reduction degradable polymeric materials that are yet to be reported. To accomplish this goal, the present investigation is aimed to develop disulfide linkage containing polyesters based on natural L-amino acid resources. By combining the melt polycondensation (green process) and natural L-amino acid (bioresources), the present approach becomes unique in making polymeric materials with reduction degradability, biocompatibility, and ability to produce supramolecular helical structures in a single polymeric system. This concept is shown in Figure 1.

The present investigation is emphasized to design and develop new classes of reduction responsive disulfide containing functional polyesters based on L-cystine resources. L-Cystine was suitably converted into multipurpose monomer with dicarboxylic esters and urethane functional groups. Earlier, we have reported dual ester-urethane condensation approach for L-amino acid based linear poly(ester-urethane)s, hyperbranched poly(ester-urethane)s, and functional polyesters.[42–45] Based on this experience, in the present investigation, melt polycondensation is successfully developed for multi-functional L-cystine monomer to make new disulfide containing polyesters (see Fig. 1). The novelty of the approaches may be listed as: (i) the dicarboxylic esters of the L-cystine monomer underwent thermoselective transesterification without disturbing the disulfide and urethane functionality to produce new classes of main chain disulfide linear polyesters, (ii) the disulfide linkages in the polyester backbone was readily susceptible to reductive degradation into small molecular species, (iii) the side chain urethane functionality facilitated β-sheet hydrogen bonding interaction among the polymer chains and seeded them for helical amyloid-fibril morphology, and (iv) on deprotection of the urethane into -$NH_3^+ X^-$, the polyester turned into non-toxic, biocompatible, and water soluble cationic species. The reductive degradation behaviors of disulfide polyester were studied using DTT and the process was monitored by ^{1}H-NMR and Gel permeation chromatographic (GPC) techniques. The self-assembly of the polymers were tested by CD spectroscopy, dynamic light scattering (DLS), atomic force, and electron microscopes. The cytotoxicity of the polymers was studied in MCF-7 cell lines and the results revealed that these cationic disulfide polymers are highly biocompatible and non-toxic to cells up to 50 μg/mL. The newly developed L-cystine polymers are completely degradable under reduction process and biocompatible for many futuristic biomedical applications.

EXPERIMENTAL METHODS

Materials

L-Cystine, 1, 12-dodecandiol, 1, 10-decanediol, 1, 8-octanediol, dithiothreitol (DTT), 1-decanol and titanium tetrabutoxide ($Ti(OBu)_4$, tetrazolium salt: 3-4,5 dimethylthiazol-2,5diphenyltetrazolium bromide (MTT), DMSO, hoechst, and 4% paraformaldehyde purchased from Aldrich chemicals and used without further purification. Methyl chloroformate, Ditertbutyldicarbonate, thionyl chloride, and other solvents were purchased locally and purified prior to use.

General Procedures

^{1}H and ^{13}C-NMR were recorded using 400-MHz JEOL NMR spectrophotometer. All NMR spectra were recorded in $CDCl_3$ containing TMS as internal standard. FT-IR spectra of all compounds were recorded using Bruker alphaT Fourier transform infrared spectrophotometer. The mass of the monomers were analzsed using a HRMS-ESI-Q-time-of-flight LCMS (SynaptG2, Waters). GPC analysis which was performed using Viscotek VE 1122 pump, Viscotek colum T6000M General mixed org 300 × 8.0 mm (THF), Viscotek VE 3580 RI detector and Viscotek VE 3210 UV/Vis detector in tetrahydrofuran (THF) using polystyrene as standards at 25 °C. Thermal stability of the polymers was determined using Perkin Elmer thermal analyzer STA 6000 model at a heating rate of 10 °C/min in nitrogen atmosphere. Thermal analysis of all polymers was performed using TA Q20 Differential Scanning Calorimeter. The instrument was calibrated with Indium standards. All the polymers were heated to melt before recording their thermograms to remove their previous thermal history. Polymers were heated and cooled at 10 °C/min under nitrogen atmosphere and their thermo grams were recorded. Circular dichroism (CD) analysis of the polymer samples was done using JASCO J-815 CD spectrometer at 20 °C in THF and water. FE-SEM images were recorded using Zeiss Ultra Plus scanning electron microscope. For FE-SEM analysis, the samples were prepared by drop casting on silicon wafers and coated with gold. Atomic force microscope (AFM) images were recorded by drop casting the samples on freshly cleaved mica surface, using Veeco Nanoscope IV instrument. The experiment was done in tapping mode.

Synthesis of Dimethyl 3, 3′-Disulfanediylbis (2-((tert-butoxycarbonyl) amino) propanoate) (Monomer 1)

To a suspension of L-cystine (19.8 g, 0.082 mol) in methanol (200 mL), thionylchloride (20.4 mL, 33.4 g, 0.283 mol) was added drop wise at 0 °C under nitrogen atmosphere.The above reaction mixture was brought to room temperature and refluxed for 12 h under nitrogen. Methanol and the unreacted thionylchloride were removed by distillation following which the solid mass was dissolved in triethylamine (46 mL, 33.7 g, 0.333 mol) and dichloromethane (200 mL) mixture at 0 °C. To the reaction mixture, Boc anhydride (41.0 mL, 41.1 g, 0.191 mol) was added drop wise at 0 °C. It was brought to 25 °C and stirring was continued for 12 h. The reaction mixture was poured into water and then extracted with dichloromethane. The organic layer was dried over anhydrous Na_2SO_4 and the solvent was removed to obtain white solid as product. It was further purified by passing through silica gel column using ethyl acetate and pet ether (1:4 v/v) as eluent. Yield = 25.1 g (65%). ^{1}H-NMR (400 MHz, $CDCl_3$) δ ppm: 5.41 (b, 2H, -NH), 4.60 (m, 2H, CH), 3.77 (s, 6H, $CHCOOCH_3$), 3.17 (m, 4H, CH_2S), and 1.45 (s, 18H, -NHCOO $(CH_3)_3$). ^{13}C-NMR (100 MHz, $CDCl_3$) δ ppm: 171.15, 155.04, 80.30, 52.82, 52.69, 52.62, 41.33, 41.26, and 28.30. FT-IR (cm^{-1}): 3743, 3364, 2938, 1749, 1682, 1509, 1363, 1216, 1163, 1057, and 1017. HRMS (ESI+): m/z [M + Na^+] calcd. for $C_{18}H_{32}N_2O_8S_2Na$ [M^+]: 491.1498; found: 491.1577.

Synthesis of Disulfide Containing Polyester (P-X) by Melt POLYCONDENSATION PROCESS

L-Cystine monomer 1 (0.67 g, 0.001 mol), 1, 12-dodecanediol (0.29 g, 0.001 mol, for polymer P-12), and benzoquinone (catalytic amount, 2.0 mg) were taken in a test tube-shaped polymerization vessel and melted in oil bath at 100 °C. The polycondensation apparatus was made oxygen and moisture free by purging with nitrogen and consequent evacuation by vacuum under constant stirring. Titanium tetrabutoxide (0.005 g, 0.01 mmol, 1.0 mol %) was added as catalyst and the melt polycondensation was carried out at 120 °C for 4 h with constant stirring under nitrogen purge. During this stage, the methanol was removed along with the purge gas and the polymerization mixture became viscous. The viscous melt was further subjected to high vacuum (0.01 mm of Hg) at 120 °C for 2 h under stirring. At the end of the polycondensation, the polymer was obtained as transparent resin. Yield =0.67 g (82%). ^{1}H-NMR (400 MHz, $CDCl_3$) δ ppm: 5.43 (b, 2H, NH), 4.60 (m, 2H, CH), 4.17 (t, 4H, CH_2COOCH_2), 3.15 (m, 4H, CH_2S), 1.70 (m, 4H, CH_2), 1.47 (s, 18H, -NHCOO $(CH_3)_3$), and 1.30 (m, 16H, CH_2). ^{13}C-NMR (100 MHz, $CDCl_3$) δ ppm: 170.72, 155.06, 80.19, 65.97, 53.08, 41.47, 29.43, 29.19, 28.49, 28.33, and 25.82. FT-IR (cm^{-1}): 3743, 3377, 2925, 2859, 1709, 1503, 1363, 1163, and 1057.

Similarly, L-cystine monomer 1 was polymerized with 1,8-octanediol and 1,10-decanediol to produce P-8 and P-10, respectively. NMR data and the molecular weights for these polymers are provided in the Supporting Information.

Model Reaction Studies

1-decanol (0.35 g, 0.002 mol) and L-cystine monomer (0.33 g, 0.001 mol) were taken in a test tube shaped polymerization apparatus and melted by placing in an oil bath at 100 °C with constant stirring. After degassing, $Ti(OBu)_4$ (0.003 g, 1 mol%) was added and the condensation was carried out at 120 °C under nitrogen purge for 4 h. At the end of the condensation reaction, the product was obtained as viscous liquid. ^{1}H-NMR (400MHz, $CDCl_3$) δ ppm: 5.43 (b, 2H, -NH), 4.61 (m, 2H, CH), 4.17 (m, 4H, $COOCH_2$), 3.18 (d, 2H, CH_2), 1.68 (m, 4H, CH_2), 1.47 (s, 18H, -NHCOO $(CH_3)_3$), 1.28 (m, 28H, CH_2), and 0.88 (t, 6H, CH_3). ^{13}C-NMR (100 MHz, $CDCl_3$) δ ppm: 170.71, 155.05, 80.19, 53.07, 41.53, 31.88, 29.53, 29.49, 29.29, 29.21, 28.48, 28.33, 25.85, 22.67, and 14.09. FT-IR (cm^{-1}): 3324, 2928, 2856, 1709, 1515, 1459,

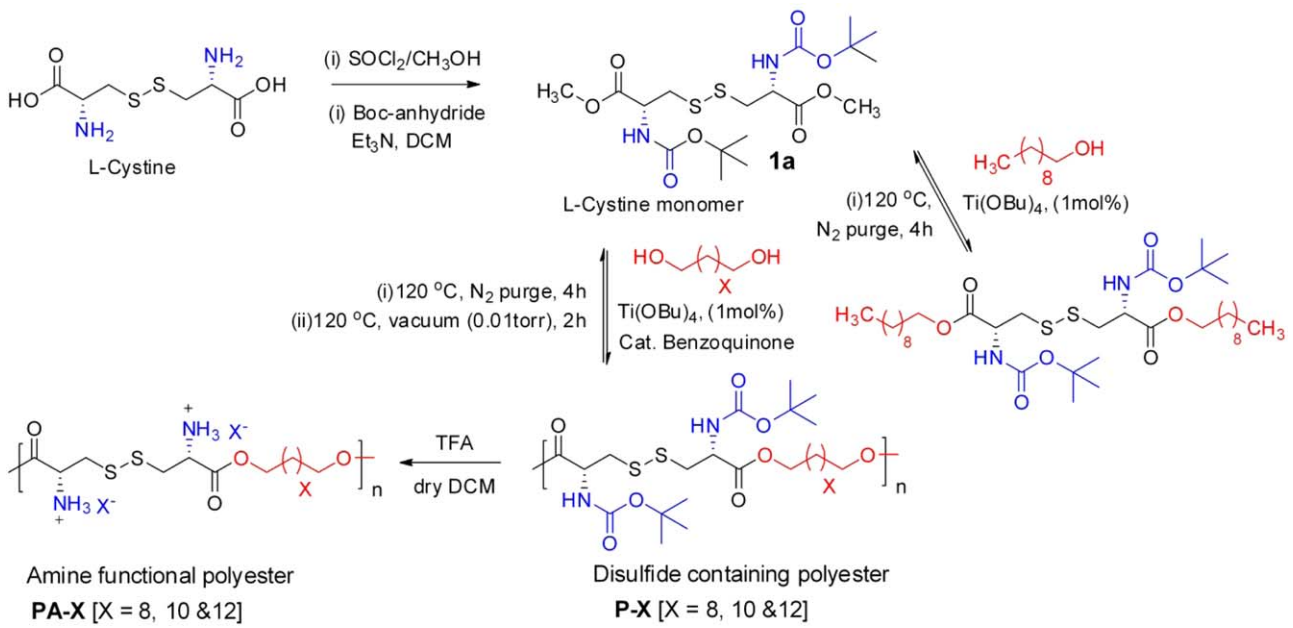

SCHEME 1 Synthesis of disulfide functional monomer 1, model compound, and polymers P-X. [Color figure can be viewed in the online issue, which is available at wileyonlinelibrary.com.]

1451, 1193, and 1047. MALDI-TOF MS: m/z [M + Na^+] calcd. for $C_{36}H_{68}N_2O_8S_2Na[M^+]$= 743.4315; Found = 743.5544.

Deprotection of Boc polymer (PA-X)

The disulfide polymer P-12 (0.81 g, 0.001 mol) was taken in a 50 mL single neck RB flask and then 5 mL of dry DCM was added into it. At 0 °C trifluoroacetic acid (TFA) (1.33 g, 1.1 mL, 0.012 mol) was added dropwise, the content was brought to 25 °C and the stirring was continued for 1 h. The solvent and TFA was removed by rotavapor and the product was purified by precipitation in cold diethyl ether. Yield = 0.59 g (89%). ^{1}H-NMR (400 MHz, CD_3OD) δ ppm: 4.38 (m, 2H, C**H**), 4.19 (m, 4H, COOC**H$_2$**), 3.26 (d, 4H, C**H$_2$**), 1.63 (m, 4H, C**H$_2$**), and 1.28 (m, 16H, C**H$_2$**).^{13}C-NMR (100 MHz, $CDCl_3$) δ ppm: 168.43, 66.58, 61.20, 51.52, 40.22, 32.81, 29.41, 29.11, 28.24, 27.91, 27.75, 27.62, 25.86, 25.65, and 25.23. FT-IR (cm^{-1}): 2927, 2856, 1750, 1661, 1532, and 1137.

Similarly, the deprotection of P-10 and P-8 polymers and their details are provided in the Supporting Information.

Degradation study

The disulfide polymer (P-12) (0.10 g, 0.0001 mol) and DTT (0.25 g, 0.001 mol) were taken in dry THF (10 mL) in 50 mL two neck round bottom flask. The polymer solution was refluxed at 70 °C and aliquots were taken periodically. The aliquots were analyzed by GPC and ^{1}H-NMR to estimate the extent of degradation.

Cell Viability Assay (MTT Assay)

Tetrazolium salt 3-(4,5 dimethylthiazol)−2,5-diphenyl tetrazolium bromide (MTT) was used in an assay to determine the cytotoxic effects of the polymer **PA-8 and PA-10** in MCF-7 cell lines. 1×10^3 cells were seeded in each well of a 96- well plate (Corning) having 100 μL of DMEM with 10% FBS (fetal bovine serum) and the cells were incubated at 37 °C under CO_2 environment for 16 h. Media was aspirated from each well and various concentrations of polymer **PA-8 and PA-10** were prepared in 100 μL of DMEM with FBS and were given to the cells. Along with polymer samples blank control of media alone was maintained in triplicates. The cells were further incubated for 72 h without changing the media. A fresh sample of MTT in sterile PBS (5 mg/mL) was prepared and diluted to 50 μg/mL in 100 μL of DMEM with FBS and this was added to each well. Cells were then incubated with MTT for 4 h at 37 °C. The media was aspirated and purple formazan crystals were obtained. These crystals were generated as a result of reduction of MTT by mitochondrial dehydrogenase enzyme from live cells. These were dissolved in 100 μL DMSO. The 96-well plate was shook for 2 min and the absorbance from formazan crystals (dissolved in DMSO) was measured using microplate reader at 570 nm (Varioskan Flash). The absorbance obtained from each well was representative of the number of cells viable per well. The mean of absorbance values were calculated for the corresponding polymer and control and that of blank control samples was subtracted from the average of treated samples. The values obtained from the control samples were taken as 100% and relative percentage values for the samples were calculated accordingly.

RESULTS AND DISCUSSION

Synthesis of Disulfide Functional Polyester

The L-cystine amino acid contains two carboxylic acids and an amine functional group with the disulfide bond. L-Cystine amino acid carboxylic acid functional groups were converted

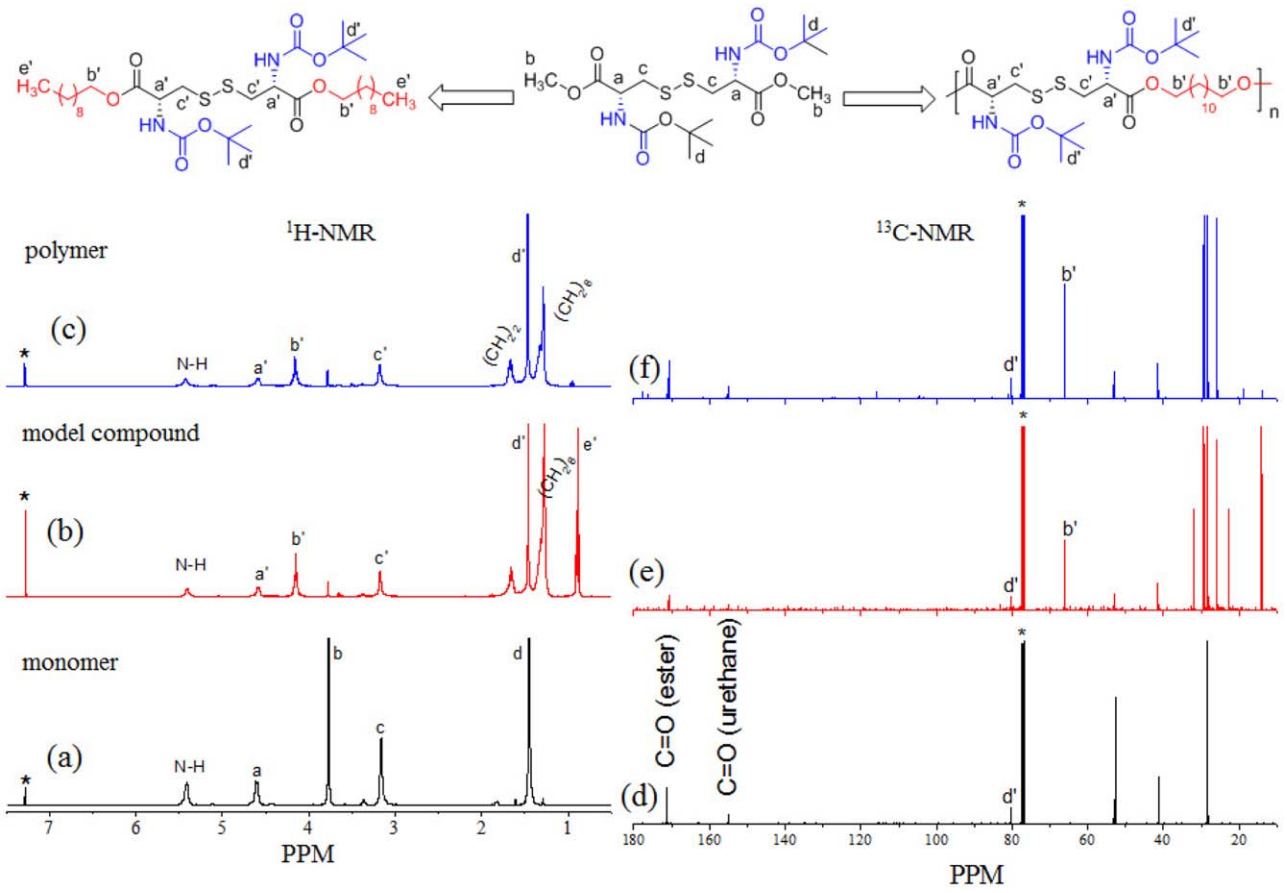

FIGURE 2 ^{1}H and ^{13}CNMR spectra of L-cystine monomer 1 (a and d), model compound (b and e), and polymer P-1 2 (c and f) in CDCl3. [Color figure can be viewed in the online issue, which is available at wileyonlinelibrary.com.]

into L-cystine methyl ester using thionyl chloride in methanol under nitrogen atmosphere. Furthermore, the amine salt was reacted with Boc anhydride to yield the L-cystine ester-urethane monomer 1 (see Scheme 1). The thermal gravimetric analysis (TGA) of L-cystine monomer 1 confirmed that it was thermally stable up to 190 °C and could be used for solvent free melt polycondensation (see SF-1). Based on our earlier expertise in the thermoselective polymerization of L-amino acid polymers,[43] the polycondensation temperature was chosen as 120 °C for the present case and $Ti(OBu)_4$ (1 mole %) was used as catalyst. Under these conditions, the ester functional group in the custom designed monomer 1 was expected to undergo thermoselective polymerization with diol to produce linear polyester without disturbing the urethane pendant in each repeating unit (the urethane functional group was completely inert toward alcohol at 120 °C).[43] To test the thermoselective polymerization of monomer 1 toward alcohol, a model reaction was performed with 1-decanol at 120 °C using Ti $(OBu)_4$ catalyst. One equivalent of L-cystine monomer 1 and two mole equivalents of 1-decanol were subjected to melt polycondensation reaction at 120 °C under nitrogen purge for 4 h. A pinch of hydroquinone was added in the polymerization mixture as radical quencher to avoid the cleavage of disulfide linkages during the melt condensation. ^{1}H-NMR and ^{13}C-NMR spectra of the monomer 1, model compound and polymers are shown in Figure 2 and the protons in the chemical structures are *assigned by alphabets*.

The L-cystine monomer COO**CH_3** ester peak at 3.65 ppm (proton b) [see Fig. 2(a)] was disappeared in the model reaction [see Fig. 2(b)] and new ester peak belongs to R-COO**CH_2**CH_2 appeared at 4.14 ppm (proton b′) [see Fig. 2(b)]. Under this reaction condition, the peak corresponding to Boc proton NHCOOC-**$(CH_3)_3$** was retained at 1.41 ppm (proton d) without any disturbance. Similarly, ^{13}CNMR spectra showed the disappearance of the ester carbon atom –O**C**H_3 at 53.45 ppm [see Fig. 2(d)] and the formation of new peak belongings to R-COO**C**H_2CH_2- at 65.01 ppm [see Fig. 2(e)]. The peak with respect to carbon atom in Boc group NHCOO**C**$(CH_3)_3$ in the monomer at 80.04 ppm was retained in the model compound [see Fig. 2(e)]. The model compound was further subjected to MALDI-TOF analysis and its spectra showed the formation of peak at m/z =743.5 (Na+) as expected for the formation of bis-ester product with Boc urethane substitutions (see SF-2). This confirmed that the Boc urethane was completely inert in the polymerisation process at 120 °C toward alcohols and only the carboxylic esters underwent transesterification to produce new ester linkages. The polymerization was carried out for equimolar

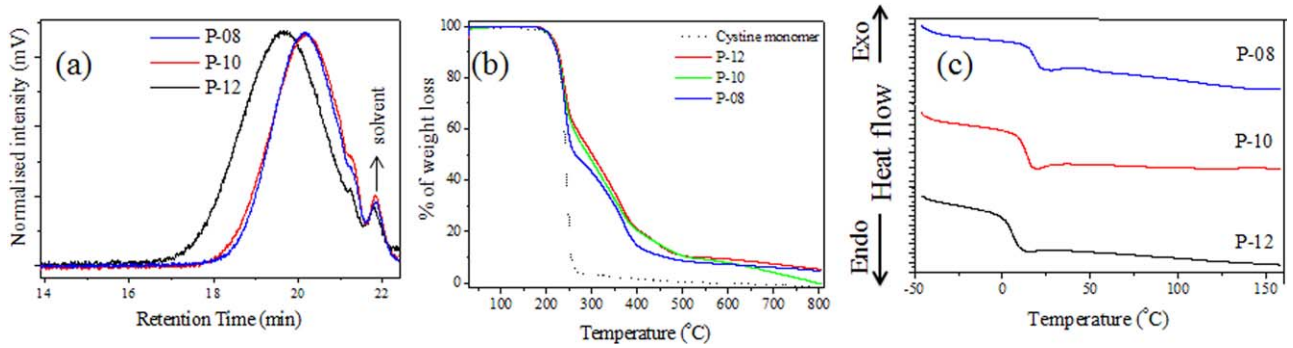

FIGURE 3 (a) GPC chromatograms of P-X polymers in THF. (b) TGA plots of the P-X polymers recorded at 10 °C/min heating rate. (c) DSC thermograms of P-X at 10°/min heating rate. [Color figure can be viewed in the online issue, which is available at wileyonlinelibrary.com.]

amounts of monomer 1 with diol in presence of $Ti(OBu)_4$ catalyst at 120 °C. For this purpose, three commercial diols 1,8-octanediol, 1,10-decanediol, and 1,12-dodecanediol were chosen. The initial polymerization under nitrogen purge for 4 h produced viscous mass which was further subjected to vacuum (0.01torr) to afford high molecular weight polymers. The L-cystine-based polymers were referred to as P-x, where x represents the number of aliphatic carbon present in the diol (see Scheme 1). The structures of the polymers were confirmed by ^{1}H and ^{13}C-NMR as shown in Figure 2(c,f) (see spectra for other polymers given in SF-3 and SF-4). The polymers showed the formation of new ester peaks in their respective NMR spectra. Furthermore, the Boc peaks were retained in the polymers as explain for model compound; thus, the thermoselective polymerization of carboxylic esters in the monomer unit produced disulfide containing functional polyesters having Boc urethane as pendants.

The molecular weight of disulfide functional polyesters were analyzed by GPC in THF as solvent. The GPC chromatograms of the disulfide functional polymers showed mono modal distribution [see Fig. 3(a)]. The molecular weights polyesters were obtained in the range of moderate to high molecular weight polymer. The molecular weights of the polymers synthesized using longer diols were found to be much higher than shorter ones (see Table 1). This trend was attributed to the steric effect introduced by the Boc group in the polymer backbone. For example, the polymers made from shorter diols are bound to have bulky Boc urethane groups at closer vicinity which are expected to induce more steric hindrance in the backbone. TGA of the disulfide functional polyesters was carried out at 10 °C/min heating rate. TGA plots in Figure 3(b) showed two distinct decomposition temperatures. First step is attributed to the decomposition of side chain Boc functional group at 220–240 °C[46,47] and the second step above 300 °C with respect to the polymer backbones [see Fig. 3(b)]. Differential scanning calorimetry (DSC) studies showed that all the disulfide polyesters were amorphous in nature [see Fig. 3(c)]. The glass transition temperature (T_g) of the polymers were increased with decrease in the spacer length of diol. Thus, the newly designed L-cystine monomer is very good in producing thermally stable disulfide containing polyester under solvent free melt polymerization process.

SELF-ASSEMBLY OF NEUTRAL AND CATIONIC POLYESTERS

The side chain Boc group in the polymers was selectively deprotected without disturbing the polyester backbone using TFA. In this process, a new cationic functionalized disulfide polyester as shown in Scheme 1. The deprotection of Boc group was confirmed by ^{1}H-NMR and FT-IR spectroscopy as shown in Figure 4. The peak belongs to $-NH(COO(CH_3)_3)$ proton at 1.41 ppm completely disappeared on deprotection without changing the polymer backbone. The FT-IR spectra of P-12 showed –NH stretching vibration band at $\nu = 3350\ cm^{-1}$ with respected to –NH bond involved in the hydrogen bonding interaction[48,49] Similarly, the $-C=O$ stretching vibration band at $\nu = 1722\ cm^{-1}$ was observed for hydrogen bonding interaction [see Fig. 4(c)]. The deprotected cationic functional polyester (amine salt $NH_3^+ X^-$) did not show peak above 3000 cm^{-1} due to the lack of NH-hydrogen bonding interactions [see Fig. 4(d)].[50,51] Based on

TABLE 1 The GPC Molecular Weights and Thermal Properties of the Polymers P-X

Sample	M_n[a] (g/mol)	M_w[a] (g/mol)	M_w/M_n[a]	T_g[b] (°C)	T_D[c] (°C)
P-8	4,100	8,400	2.1	18.6	260
P-10	6,500	16,300	2.5	14.1	262
P-12	10,400	31,500	3.0	6.2	268

[a] The molecular weights were determined by GPC in THF solvent.
[b] T_g was obtained from DSC at 10 °C/min heating rate.
[c] T_D was obtained from TGA for 5% weight loss and at 10 °C/min heating rate.

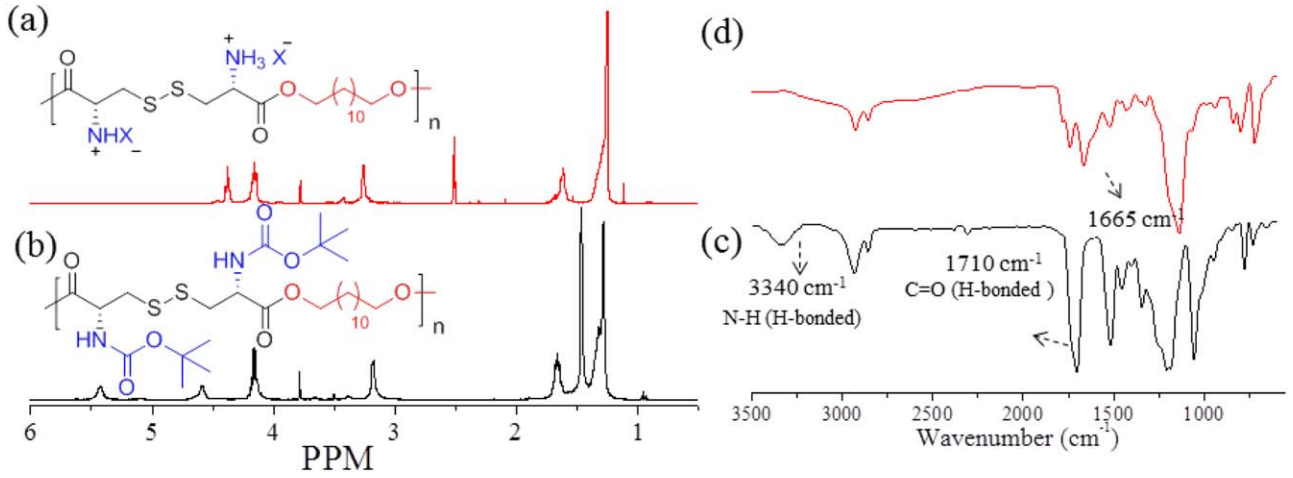

FIGURE 4 ^{1}HNMR (a) and FT-IR spectrum (c) of P-12. ^{1}HNMR (b) and FT-IR spectrum (d) of the deprotected cationic polymer PA-12. [Color figure can be viewed in the online issue, which is available at wileyonlinelibrary.com.]

the above studies, it can be concluded that the new synthetic approach is very useful for making cationic functionalized polyester based on L-cystine amino acid resources.

The custom designed L-cystine functional polyesters were subjected to self-assembly studies in organic solvents and water. The Boc pendant polyester was found to be insoluble in water; thus, their self-assembly studies were carried out in THF. Conversely, the deprotected cationic polymer was found to be dispersible in water. The cationic polymer was dissolved in DMSO + water mixture (1: 1 v/v) and the solution was transferred to semi-permeable membrane. It was dialyzed against large amount of water for 24 h with constant replenishing of fresh water at regular interval. The dialyzed polymer solution was found to be stable for more than a month. The disulfide functional polyester are made up of optically active L-cystine amino acid as the starting material; hence both the neutral polymer (having Boc pendent) and cationic polymer were subjected to CD analysis to determine their secondary structures (see Fig. 5). CD spectra of the neutral polymer showed broad negative CD band at 260 nm and positive CD band at 220 nm with respect to β-sheet conformation [see Fig. 5(a)].[52,53] The CD spectra showed broad signal from 250 to 280 nm. The cationic polymer was subjected for CD analysis in both water and THF [see Fig. 5(b,c)]. CD spectra of the cationic polymer showed positive CD around 220 nm in both THF and water with respect to random coil conformation.[52,53] The disappearance of the β-sheet conformation in the cationic polymer was attributed to the lack of the hydrogen bonding in their $NH_3^+ X^-$ amine salt. This was further confirmed by the FT-IR analysis [see Fig. 4(c,d)] that the neutral polymer exhibited strong β-sheet hydrogen bonding whereas the cationic polymer lack hydrogen bonding in their $NH_3^+ X^-$ amine salt.[48,49]

The aqueous dialyzed cationic polyester samples were subjected to DLS as well as zeta potential analysis. DLS histograms of the polymers in Figure 6(a–c) showed mono-modal distributions with hydrodynamic diameter of 160–220 nm ± 20 nm. The DLS studies revealed that the disulfide cationic polyesters self-assembled as stable nanoparticles in water. The polyester backbone is relatively rigid and hydrophobic in nature. The cationic NH_3^+ units in the side arm are hydrophilic and are easily surrounded by water molecules. As a result, the cationic polyesters became amphiphilic in nature and self-assembled into spherical nanoparticles. This was

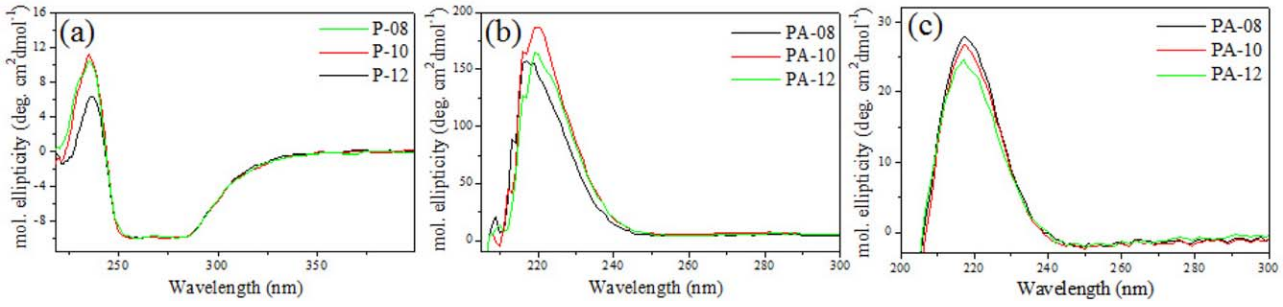

FIGURE 5 (a) CD Spectra of neutral polymer P-X in THF. CD Spectra of cationic polymer PA-X in THF (b) and its dialyzed polymer sample PA-X in water (c). [Color figure can be viewed in the online issue, which is available at wileyonlinelibrary.com.]

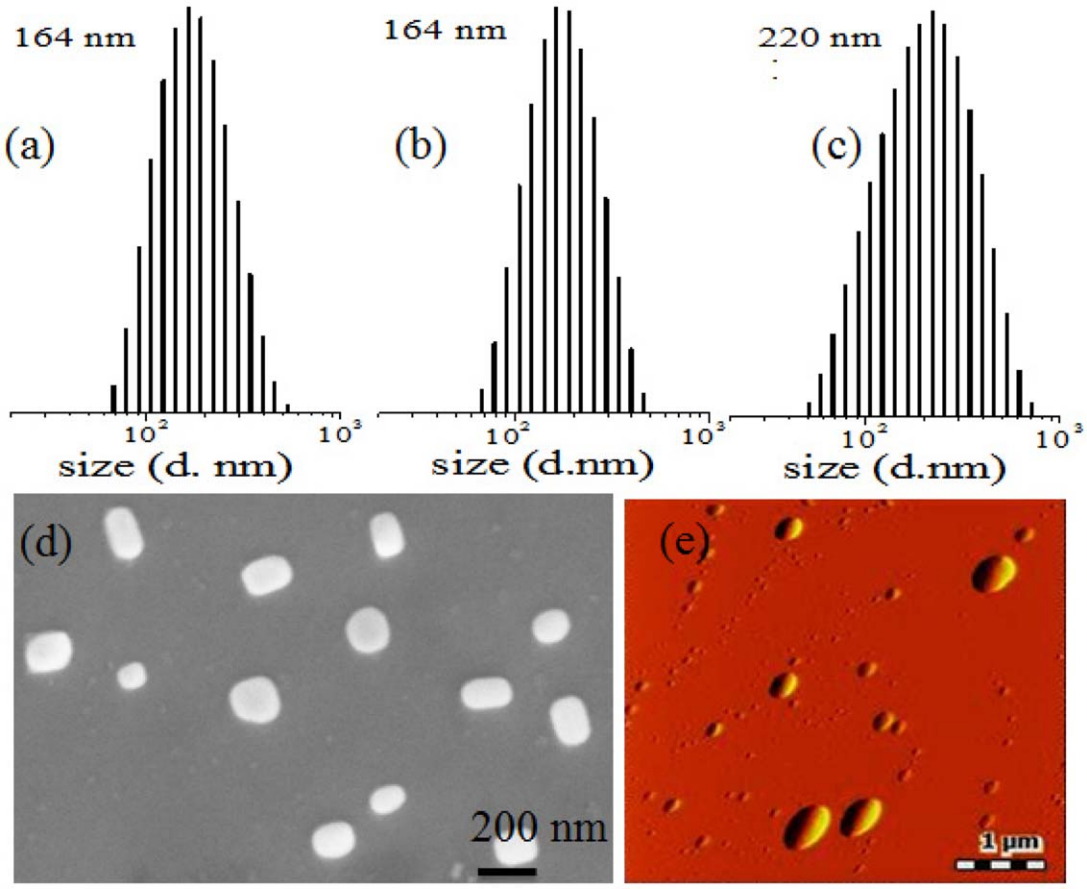

FIGURE 6 DLS histograms of dialyzed cationic polymer sample PA-8 (a), PA-10(b), and PA-12(c). FE-SEM (d) and AFM images of the cationic PA-12 polymer (e). The concentration of the polymer was retained as 0.1 mg/mL for DLS measurements. [Color figure can be viewed in the online issue, which is available at wileyonlinelibrary.com.]

further proved by the Zetapotential measurements of the cationic polyesters (see SF 5). The cationic polymers showed a positive voltage of 5 mV corresponding to the positive charges at the periphery of the nanoparticles. To identify the morphology of the cationic polymer, dialyzed PA-12 sample was subjected to FE-SEM and AFM analysis. FE-SEM images showed the formation of spherical nanoparticle of 200 ± 25 nm in diameter [see Fig. 6(d)] (for more FE-SEM images see SF 6). Furthermore, AFM analysis also showed the spherical nanoparticle morphology with diameters of 200 ± 20 nm [see Fig. 6(e)] (for more AFM images see SF 6). The sizes of the nanoparticles from FE-SEM and AFM analysis were well matched with the solution aggregates subjected to DLS analysis indicating that these cationic polymers indeed existed as spherical nanoparticle in water.

Since the disulfide neutral polyester showed β-sheet signals in the CD spectra (in THF); they were subjected to FE-SEM and AFM microscopic analysis. The FE-SEM images of the dropcast films are shown in Figure 7(a–c). The disulfide neutral polyester P-8, P-10, and P-12 exhibited amyloid-like nanofibril morphologies (for more FE-SEM images see SF 7 - SF 9). The thickness of the nanofibrils was obtained as 75 ± 13 nm and the length of the fiber varied up to few micrometres. Furthermore, the fibrils were found to exhibit left-handed twists with respect to their β-sheet signal in CD spectra (negative cotton effect). AFM images of disulfide neutral polyesters are shown in Figure 7(d–f). AFM images exhibited nanofibrous morphology as observed in the FE-SEM (for more AFM images see SF 10). The thickness of the nanofibrils was found to be in the range of 69 ± 12 nm with length up to few micrometres. Thus, FE-SEM and AFM analysis confirmed that the nanofibrous morphology of the disulfide neutral polyesters (P-X). Based on the FE-SEM, AFM, and CD analysis of the polymers the following conclusion can be arrived: (i) the disulfide containing Boc pendent neutral polymer adopted expanded chain conformation in organic solvent and produced helical amyloid-fibrils morphology, (ii) the deprotection of Boc group resulted in the formation new disulfide linkage containing cationic polyester, and (iii) the cationic polyester adopted random-coil conformation and self-assembled as spherically charged nanoparticles in water.

REDUCTION DEGRADATION AND CYTOTOXICITY

To study the reduction cleavages of the disulfide bond in polyester backbone,[19] the polymer P-12 was subjected to degradation using DTT as a reducing agent. The degradation of

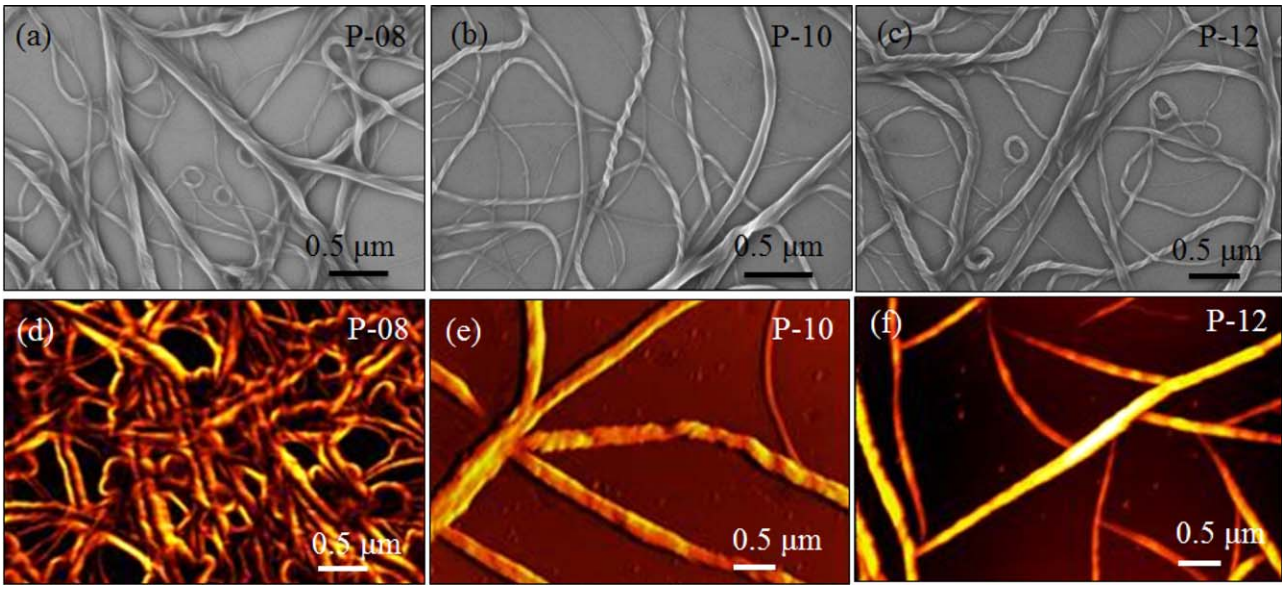

FIGURE 7 SEM images of disulfide functional polyesters (P-X) (a–c) and AFM images of P-X (d–f). The concentration of polymer was maintained for microscopic analysis (0.1 mg/mL). [Color figure can be viewed in the online issue, which is available at wileyonlinelibrary.com.]

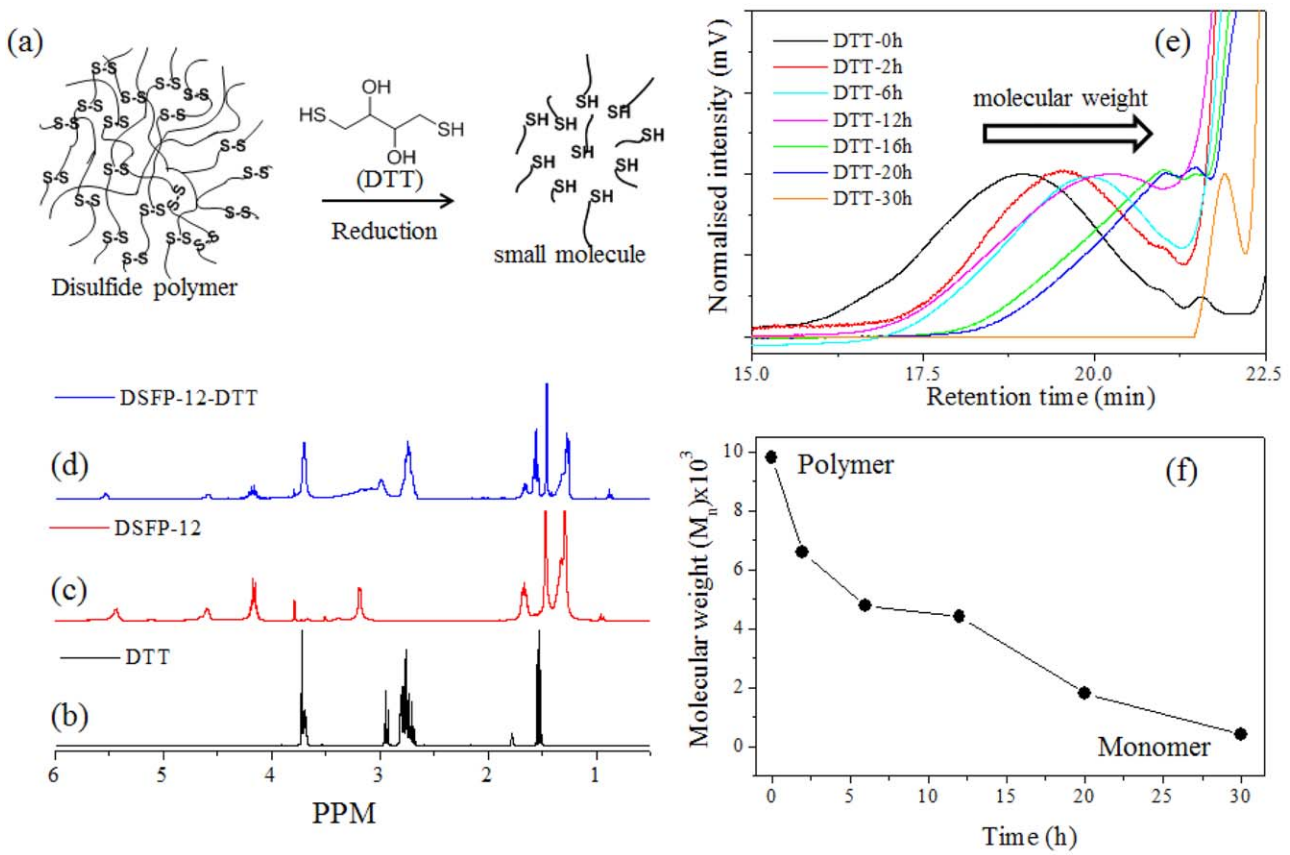

FIGURE 8 Representation of disulfide polymer degradation by DTT (a). ^{1}HNMR stack plot for DTT (b), disulfide polymer (c), and DTT degraded disulfide polymer (d). GPC chromatograms of degradation product aliquots (e). Plot of Mn versus degradation reaction time (f). [Color figure can be viewed in the online issue, which is available at wileyonlinelibrary.com.]

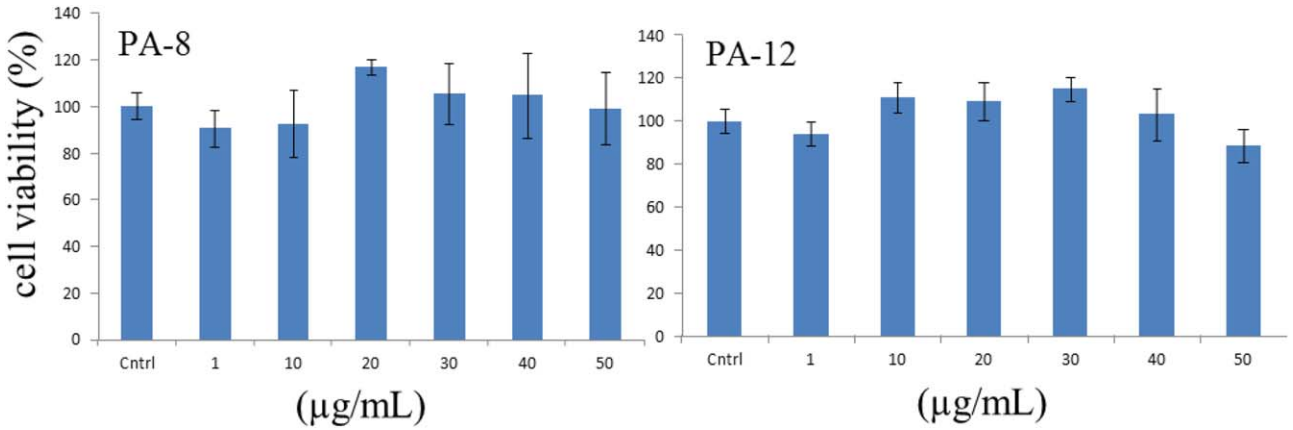

FIGURE 9 The cytotoxicity data for cationic polymers in MCF-7 breast cancer cell line. [Color figure can be viewed in the online issue, which is available at wileyonlinelibrary.com.]

disulfide functional polyester was carried out in anhydrous THF at 70 °C. The degradation of disulfide backbone by DTT is schematically shown in Figure 8(a). The degradation of disulfide polymers was studied by collecting aliquots at various time intervals and subjects them for ^{1}H-NMR and GPC studies. ^{1}H-NMR spectra of DTT, P-12, and aliquots taken from the degradation at 30 h are shown in Figure 8(b–d), respectively. The polymer showed -**CH_2**-S-S-**CH_2**- protons at 3.18 ppm [see Fig. 8(c)] which are completely disappeared in the degradation aliquot [see Fig. 8(d)]. Furthermore, new peaks corresponding to **CH_2**-SH appeared at 2.99 ppm in the degraded aliquot [see Fig. 8(d)]. This observation provided direct evidence for the disulfide linkage cleavage in the polymers by reducing agent such as DTT. The GPC chromatograms of degradation product aliquots are shown in Figure 8(e). At the beginning, the disulfide polymers showed peak maxima at 18 min; on degradation, the GPC chromatogram shifted toward the higher retention time with respect to the low molecular weight chains. These studies clearly indicated that the high molecular weight disulfide polymer chains were degraded in presence of DTT into lower molecular weight oligomers. The plot of M_n versus reaction time for all the aliquots is shown in Figure 8(f). The number average molecular weight (M_n) of the degraded product showed a drastic decrease from 10.0×10^3 g/mol to 500 g/mol (monomer or dimer species). Based on study, it may be conclude that the custom designed disulfide containing polyesters are readily susceptible to reductive cleavage. Hence, these neutral polyester materials could be useful for wide range of applications in thermoplastic industry. Furthermore, the aqueous nanoassemblies of the cationic polymer samples could be used for biomedical applications such in drug delivery and so on.

The cytotoxicity of the cationic disulfide amine polyesters were investigated in breast cancer (MCF-7 cells) cell lines using MTT assay method. The concentration of the polymers (PA-8 and PA-10) was varied from 1 to 50.0 μg/mL. The cytotoxicity of the polymer (see Fig. 9) showed that the amino acid-based cationic disulfide amine polymers were found to be non-toxic to cancer cells up to 50.0 μg/mL concentration with $>95\%$ of cell viability. These results revealed that these polymers are highly biocompatible in nature; hence, it can be used for biomaterial and biomedical applications. There are large numbers of cationic polymer nanoparticles are currently investigated for DNA and SiRNA delivery in cancer therapy.[54–56] Furthermore, the cationic nanoparticles are proved to be enhancing the cell adhesion via columbic interactions and facilitated the uptake of the drug loaded polymer scaffolds.[57] Thus, the custom designed cationic polyester nanoparticles are important classes of biomaterials for polymer drug delivery applications in cancer therapy. Currently, we are in the process of fine-tuning the chemical structures of the polymers to enhance their anticancer drug loading and delivery to cancer cells.

CONCLUSION

In conclusion, solvent free melt polycondensation method was developed for redox degradable disulfide functional polyester based on L-cystine amino acid. The ester group of the L-cystine monomer reacted with various aliphatic diols in the presence of $Ti(OBu)_4$ as catalyst to yield disulfide functional polyester under solvent free melt condition. In this method, the ester functional group selectively underwent reaction with diol at these particular reaction condition and the urethane group was remained absolutely inert. The formation of disulfide functional polyesters was confirmed by NMR spectroscopy. The functional polyesters produced moderate to high molecular weight polymers. CD analysis of neutral disulfide functional polyester exhibited β-sheet secondary structure whereas its deprotected cationic disulfide functional polyester showed random coil secondary structure. Microscopic analysis revealed the formation of amyloid-like fibrous assembly for neutral disulfide polyester and spherical particle morphology for water soluble cationic polyester. The above results indicated that the structural differences between Boc-protected and free amine in the polymer side chain easily fine-tuned to change the morphology from amyloid fibres to particles. The cell viability of cationic amine functional polymers in MCF

cells showed upto 50 μg/mL of polymer are viable (non-toxic) and these polymers are biocompatible in nature. The neutral (Boc) disulfide functional polyesters on degradation using DTT as the reducing agent converts a high molecular weight polymer into small molecular weight fragments indicating their importance as stimuli responsive polymers in future biomaterials application.

ACKNOWLEDGMENTS

The authors thank research grant from Department of Science and Technology (DST), New Delhi, INDIA, under SERB scheme SB/S1/OC-37/2013. S. Anantharaj thanks CSIR New Delhi for Ph.D. research fellowship.

REFERENCES AND NOTES

1 G. L. Fiore, S. J. Rowan, C. Weder, *Chem. Soc. Rev.* **2013**, *42*, 7278–7288.

2 E.-K. Bang, M. Lista, G. Sforazzini, N. Sakai, S. Matile, *Chem. Sci.* **2012**, *3*, 1752–1763.

3 J. A. Syrett, C. R. Becer, D. M. Haddleton, *Polym. Chem.* **2010**, *1*, 978–987.

4 H. Colquhoun, B. Klumperman, *Polym. Chem.* **2013**, *4*, 4832–4833.

5 Y. Ding, A. S. Hay, *Macromolecules* **1996**, *29*, 6386–6392.

6 Y. Ding, A. S. Hay, *Macromolecules* **1997**, *30*, 2527–2531.

7 Z. A. Liang, Y. Z. Meng, L. Li, X. S. Du, A. S. Hay, *Macromolecules* **2004**, *37*, 5837–5840.

8 Y. Z. Meng, Z. A. Liang, Y. X. Lu, A. S. Hay, *Polymer* **2005**, *46*, 11117–11124.

9 L. N. Song, M. Xiao, D. Shu, S. J. Wang, Y. Z. Meng, *J. Mater. Sci.* **2007**, *42*, 1156–1161.

10 E. Q. Rosenthal, J. E. Puskasand, C. Wesdemiotis, *Biomacromolecules* **2012**, *13*, 154–164.

11 Y. Lee, H. Koo, G. Jin, H. Mo, M. Y. Cho, J. Y. Park, J. S. Choi, J. S. Park, *Biomacromolecules* **2005**, *6*, 24–26.

12 N. V. Tsarevsky, K. Matyjaszewski, *Macromolecules* **2002**, *35*, 9009–9014.

13 H. Otsuka, S. Nagano, Y. Kobashi, T. Maeda, A. Takahara, *Chem. Commun.* **2010**, *46*, 1150–1152.

14 M. Pepels, I. Filot, B. Klumperman, H. Goossens, *Polym. Chem.* **2013**, *4*, 4955–4965.

15 B. D. Fairbanks, S. P. Singh, C. N. Bowman, K.S. Anseth, *Macromolecules* **2011**, *44*, 2444–2450.

16 K. Dan, S. Ghosh, *Angew. Chem. Int. Ed.* **2013**, *52*, 7300–7305.

17 D. Basak, R. Kumar, S. Ghosh, *Macromol. Rapid Commun.* **2014**, *35*, 1340–1344.

18 R. Nicolay, L. Marx, P. Hemery, K. Matyjaszewski, *Macromolecules* **2007**, *40*, 9217–9223.

19 H. Chen, J. Jia, X. Duan, Z. Yang, J. Kong, *J. Polym. Sci., Part A Polym. Chem.* **2015**, *53*, 2374–2380.

20 J. Rosselgong, E. G. L. Williams, T. P. Le, F. Grusche, T. M. Hinton, M. Tizard, P. Gunatillake, S. H. Thang, *Macromolecules* **2013**, *46*, 9181–9188.

21 S. Pal, M. R. Hill, B. S. sumerlin, *Polym. Chem.* **2015**, *6*, 7871–7880.

22 Y. Li, S. P. Armes, *Macromolecules* **2005**, *38*, 8155–8162.

23 T. Zhao, Y. Zheng, J. Poly, W. Wang, *Nat. Commun.* **2013**, *4*, 1–8.

24 A. C. Engler, J. M. W. Chan, K. Fukushima, D. J. Coady, Y. Y. Yang, J. L. Hedrick, *ACS Macro Lett.* **2013**, *2*, 332–336.

25 S. Son, E. Shin, B.-S. Kim, *Macromolecules* **2015**, *48*, 600–609.

26 J. Canadell, H. Goossens, B. Klumperman, *Macromolecules* **2011**, *44*, 2536–2541.

27 A. Sulistio, A. Blencowe, A. Widjaya, X. Zhang, G. Qiao, *Polym. Chem.* **2012**, *3*, 224–234.

28 A. Sulistio, A. Widjaya, A. Blencowe, X. Zhang, G. Qiao, *Chem. Commun.* **2011**, *47*, 1151–1153.

29 A. Sulistio, J. Lowenthal, A. Blencowe, M. N. Bongiovanni, L. Ong, S. L. Gras, X. Zhang, G. G. Qiao, *Biomacromolecules* **2011**, *12*, 3469–3477.

30 J. R. Kramer, T. J. Deming, *Chem. Commun.* **2013**, *49*, 5144–5146.

31 J. Wu, L. Zhao, X. Xu, N. Bertrand, W. Choi, B. Yameen, J. Shi, V. Shah, M. Mulvale, J. L. MacLean, O. C. Farokhzad, *Angew. Chem. Int. Ed.* **2015**, *54*, 9218–9223.

32 N. R. Ko, J. K. Oh, *Macromolecules* **2014**, *15*, 3180–3189.

33 P. Yang, D. Li, S. Jin, J. Ding, J. Guo, W. Shi, C. Wang, *Biomaterials* **2014**, *35*, 2079–2088.

34 L. Jia, D. Cui, J. Bignon, A. D. Cicco, J. Wdzieczak-Bakala, J. Liu, M.-H. Li, *Biomacromolecules* **2014**, *15*, 2206–2217.

35 N. Song, M. Ding, Z. Pan, J. Li, L. Zhou, H. Tan, Q. Fu, *Biomacromolecules* **2013**, *14*, 4407–4419.

36 Y. Wang, J. Nie, B. Chang, Y. Sun, W. Yang, *Biomacromolecules* **2013**, *14*, 3034–3046.

37 F. Feng, R. Li, Q. Zhang, Y. Wang, X. Yang, H. Duan, X. Yang, *Polymer* **2014**, *55*, 110–118.

38 C. Ferris, M. Violante de Paz, A. Aguilar de Leyva, I. Caraballo, J. A. Galbis, *Polym. Chem.* **2014**, *5*, 2370–2381.

39 N. Chan, B. Khorsand, S. Aleksanian, J. K. Oh, *Chem. Commun.* **2013**, *49*, 7534–7536.

40 H.-C. Kim, E. Kim, S. G. Lee, S. J. Lee, H. Kim, S. W. Jeong, *J. Polym. Sci., Polym. Chem.* **2014**, *52*, 582–589.

41 G. Odian, Principles of Polymerization, 3rd ed.; Wiley: New York, **1991**.

42 S. Anantharaj, M. Jayakannan, *Biomacromolecules* **2012**, *13*, 2446–2455.

43 S. Anantharaj, M. Jayakannan, *Biomacromolecules* **2015**, *16*, 1009–1020.

44 R. Aluri, M. Jayakannan, *Polym. Chem.* **2015**, *6*, 4641–4649.

45 S. Anantharaj, M. Jayakannan, *J. Polym. Sci., Polym. Chem.* **2016**, *54*, 1065–1077.

46 M. Horie, I. Yamaguchi, T. Yamamoto, *Macromolecules* **2006**, *39*, 7493–7501.

47 J. K. Leonard, Y. Wei, K. B. Wagener, *Macromolecules* **2012**, *45*, 671–680.

48 J. Mattia, P. Painter, *Macromolecules* **2007**, *40*, 1546–1554.

49 H. Wang, S. R. Aubuchon, D. G. Thompson, J. C. Osborn, A. L. Marsh, W. R. Nichols, J. R. Schoonover, R. A. Palmer, *Macromolecules* **2002**, *35*, 8794–8801.

50 M. Llusar, G. Monros, C. Roux, J. L. Pozzo, C. Sanchez, *J. Mater. Chem.* **2003**, *13*, 2505–2514.

51 K. E. Feldman, M. J. Kade, E. W. Meijer, C. J. Hawker, E. J. Kramer, *Macromolecules* **2009**, *42*, 9072–9081.

52 A. Sinaga, T. A. Hatton, K. C. Tam, *Biomacromolecules* **2007**, *8*, 2801–2808.

53 N. Greenfield, B. Davidson, G. D. Fasman, *Biochemistry* **1967**, *6*, 1630–1637.

54 B. Z. Zhou, Y. Shen, J. Tang, M. Fan, E. A. V. Krik, W. J. Murdoch, M. Radosz, *Adv. Funct. Mater.* **2009**, *19*, 3580–3589.

55 S. S. Dunn, S. Tian, S. Blake, J. Wang, A. L. Galloway, A. Murphy, P. D. Pohlhaus, J. P. Rolland, M. E. Napier, J. M. DeSimone, *J. Am. Chem. Soc.* **2012**, *134*, 7423–7430.

56 M. Sanjoh, K. Miyata, R. J. Christie, T. Ishii, Y. Maeda, F. Pittella, S. Hiki, N. Nishiyama, K. Kataoka, *Biomacromolecules* **2012**, *13*, 3641–3649.

57 S. Wang, S. Zhang, J. Liu, Z. Liu, L. Su, H. Wang, J. Chang, *ACS Appl. Mater. Interfaces* **2014**, *6*, 10706–10713.